

Master Equation Approach to Fluctuations in a Model Excitable Spatially Extended Chemical System

B. Nowakowski and A. L. Kawczyński*

Institute of Physical Chemistry, Polish Academy of Sciences, Kasprzaka 44/52, 01-224 Warsaw, Poland

Received: February 11, 1998; In Final Form: April 9, 1998

A simple and realistic model of an excitable chemical system in which running impulses can be observed is studied. Mesoscopic characteristics of the model are obtained by numerical simulations of the master equation for spatially extended system. Velocity of the impulse and its shape obtained in the simulations agree well with the phenomenological description. For small diffusion coefficients, fluctuations grow locally and create impulses of excitations. Formation of such impulses cannot be described by the phenomenological approach. However, if an excitation is sufficiently developed, its subsequent evolution can be predicted with reasonable accuracy by phenomenological equations.

I. Introduction

In an excitable regime, a nonlinear dynamical system has only one attractor and all trajectories attend it asymptotically. In the simplest case the attractor is a stable stationary state. However, not all trajectories are directly attracted to this state. Trajectories beginning at some distance from the stable stationary state initially go away from it and only later on are they attracted back to it, whereas trajectories initialized sufficiently close to the stable stationary state are directly attracted to it. Such properties can exhibit only nonlinear dynamical systems whose behavior is governed by two or more variables. Usually, the excitable systems are close to either the Hopf bifurcation in which they switch to an oscillatory regime or to a saddle-node bifurcation in which bistability appears. There are known many chemical systems that exhibit excitability.¹ They can be excitable only in far-from-equilibrium conditions. The best known example of excitable systems is the Belousov–Zhabotinsky (B–Z) reaction. Perturbations of the stable stationary state with high concentration of the reduced catalyst by additions of small amounts of a silver ion solution can generate a rapid increase (pulse) of concentration of the oxidized form of the catalyst after which the system returns to the stationary state. In spatially extended systems, such local perturbations can lead to generation of the single impulse of concentrations spreading with a constant velocity.^{2–7} If ferroin is used as the catalyst in the B–Z reaction the running impulse is seen as the blue zone spreading through the red solution.

The dynamics of excitable systems can be sensitive to internal fluctuations. Small fluctuations around a stable stationary state are damped, but sufficiently large fluctuations can induce large deviations of concentrations from the stationary state. One can expect an important difference in the influence of fluctuations on the behavior of stirred and unstirred excitable chemical systems. An ideally stirred excitable system may be treated as homogeneous. If a size of a system is small, homogeneity can also be maintained by sufficiently fast diffusion. In an unstirred spatially extended excitable system, diffusion is not always able to disperse local fluctuations of concentrations. In this case local fluctuations can increase and form domains in which concentrations rapidly go away from the stable stationary state. These domains can grow to impulses of excitations that next expand owing to the traveling wave mechanism and cover a

substantial part of the system. We study these phenomena in the present paper using phenomenological and stochastic descriptions. In order to include local fluctuations in the description of dynamics of an excitable system we use the master equation (ME) approach,^{8–10} which accounts for stochastic character of chemical and diffusion processes. Spatially extended inhomogeneous as well as homogeneous systems at the initial instance will be considered. We extend here our previous investigations on the influence of global fluctuations on the behavior of the homogeneous (ideally stirred) excitable system.¹¹ In particular, we are concerned with the influence of diffusion on the dynamics of local fluctuations.

We want to stress that at present it is not possible to study effectively any real chemical system exhibiting excitable dynamics (like the B–Z reaction) by the master equation approach. Therefore, one must consider models as simple as possible, which can be efficiently simulated using numerical methods. Recently, we have constructed the simple but realistic chemical model that exhibits excitability¹¹ as well as oscillatory behavior¹² in homogeneous systems. In these cases only global fluctuations were taken into account. The model consists of bimolecular reactions excluding autocatalysis, and therefore it can be easily simulated by ME method as well as by molecular dynamics technique for reactive hard spheres.¹³ We consider here the same chemical scheme as in the previous papers,^{11,12} but now we include local fluctuations by considering a spatially extended system in which inhomogeneities can appear. We examine the relation between the stochastic and deterministic descriptions by comparing the results of the master equation approach with the solutions of the corresponding reaction–diffusion equations. For spatially extended systems, the ME approach has been already applied to study effects of fluctuations in models of bistable systems^{8–10,14,15} and the model with chemical kinetics described by the quadratic autocatalytic term.¹⁶ These models have been also studied by the Langevin approach, which is based on introduction of noise terms to corresponding phenomenological equations.¹⁷ Many important results concerning stochastic effects in the dynamics of explosive systems has been proved by Zel'dovich and co-workers,¹⁸ but these results have not been obtained from the ME approach. To our best knowledge there are no papers using the ME approach to excitable spatially extended chemical systems.

The paper is organized as follows: In section II the chemical scheme is described, and next a phenomenological dynamics based on reaction–diffusion equations is analyzed. In section III the master equation and the algorithm for its simulations are presented. In section IV the results are presented and discussed. Section V contains conclusions.

II. Phenomenological Model

The model consists of nine elementary (bimolecular) processes:



The reactant V is transformed to the product U with E as the catalyst (steps 2 and 3). This part of the scheme is the modification of the well-known Langmuir–Hinshelwood mechanism of catalytic reactions (or the Michaelis–Menten kinetics for enzymatic reactions). Step 4 describes the inhibition of the Langmuir–Hinshelwood mechanism (or the Michaelis–Menten scheme) by an excess of the reactant V. Moreover, the reactant V is transformed directly to the product U in the step 5. The system is open, owing to step 1, in which the reactant V is produced from the reagent R, whose concentration is maintained constant. It is assumed that S is a solvent whose concentration is also kept constant. One can arrange such conditions in a continuously fed unstirred reactor (CFUR) or a so-called “gel disc reactor”. Because we are interested in inhomogenous systems, we allow for initial distributions of reagent concentrations that depend on spatial coordinates. Therefore, local mass balance equations with reaction and diffusion terms for each reagent separately must be used to describe the dynamics of the system. According to the mass action law, the behavior of the system is described by five reaction–diffusion equations for V, U, E, X, and Y. For simplicity we restrict our considerations to one-dimensional systems. The kinetic equations have the form

$$\frac{\partial V}{\partial t} - D_V \frac{\partial^2 V}{\partial x^2} = k_1 RS - k_{-1} VS - k_2 VE + k_{-2} XS - k_4 VX + k_{-4} YS - k_5 VS + k_{-5} US \quad (6)$$

$$\frac{\partial U}{\partial t} - D_U \frac{\partial^2 U}{\partial x^2} = k_3 XS + k_4 VS - k_{-5} YS \quad (7)$$

$$\frac{\partial E}{\partial t} - D_E \frac{\partial^2 E}{\partial x^2} = -k_2 VE + (k_{-2} + k_3) XS \quad (8)$$

$$\frac{\partial X}{\partial t} - D_X \frac{\partial^2 X}{\partial x^2} = k_2 VE - (k_{-2} + k_3) XS - k_4 VX + k_{-4} YS \quad (9)$$

$$\frac{\partial Y}{\partial t} - D_Y \frac{\partial^2 Y}{\partial x^2} = k_4 VX - k_{-4} YS \quad (10)$$

where the italicized symbols of the reagents are used to denote their concentrations for convenience, because this notation does not cause any misunderstandings.

In the sequel we will assume that diffusion coefficients of all reagents are identical and equal to D . Moreover, initial distributions of a total concentration of the catalyst or the enzyme ($E(x, 0) + X(x, 0) + Y(x, 0)$) are constant in space. In this case the sum $E(x, t) + X(x, t) + Y(x, t) = E_0$ remains constant for time $t > 0$, and therefore, one of the variables (say $Y(x, t)$) can be eliminated. Thus, the dynamics of the system can be described by four reaction–diffusion equations only:

$$\frac{\partial V}{\partial t} - D \frac{\partial^2 V}{\partial x^2} = k_1 RS - k_{-1} VS - k_2 VE + k_{-2} XS - k_4 VX + k_{-4}(E_0 - E - X)S - k_5 VS + k_{-5} US \quad (11)$$

$$\frac{\partial U}{\partial t} - D \frac{\partial^2 U}{\partial x^2} = k_3 XS + k_4 VS - k_{-5} YS \quad (12)$$

$$\frac{\partial E}{\partial t} - D \frac{\partial^2 E}{\partial x^2} = -k_2 VE + (k_{-2} + k_3) XS \quad (13)$$

$$\frac{\partial X}{\partial t} - D \frac{\partial^2 X}{\partial x^2} = k_2 VE - (k_{-2} + k_3) XS - k_4 VX + k_{-4}(E_0 - E - X)S \quad (14)$$

In order to argue on possibility of running impulse solution to these equations, let us consider the case of the homogeneous system. In the previous papers^{11,12} we have shown that the corresponding kinetic equations (without the diffusion terms) have only one stationary state given by

$$V_s = \frac{R}{K_1} \quad (15)$$

$$U_s = \frac{k_3 E_0 SR}{k_2 k_{-5} (k_2 (R^2 / (K_1 K_4) + RS) + K_1 S^2 (k_{-2} + k_3))} + \frac{R}{K_1 K_5} \quad (16)$$

$$E_s = \frac{E_0 S^2 (k_{-2} + k_3)}{(R^2 / (K_1 K_4) + RS / K_1) k_2 + S^2 (k_{-2} + k_3)} \quad (17)$$

$$X_s = \frac{E_0 SR k_2}{(R^2 / (K_1 K_4) + RS) k_2 + K_1 S^2 (k_{-2} + k_3)} \quad (18)$$

where $K_i = k_{-i}/k_i$ for $i = 1, 4$, and 5 . For appropriate choice of the rate constants and the concentrations of S , R , and E_0 the stationary state is attracting. ME simulations can be performed in the efficient way if the rate constants are not very different, which means that all reactions occur at similar time scale. Also values of the diffusion coefficients have to be chosen in such a way that spreading of running impulses can be detected in reasonable intervals of time and size of the system. For the same reason, ratios of the concentrations of all reagents should not differ by many orders of magnitude. In particular, in simulations described below we have used $S = 0.1$, $R = 0.2$, $E_0 = 0.2$ and $k_1 = 0.01$, $k_{-1} = 0.012$, $k_2 = 8.0$, $k_{-2} = 0.1$, $k_3 = 3.9$, $k_4 = 1.0$, $k_{-4} = 4.0$, $k_5 = 0.1$, $k_{-5} = 0.1$. Two values of the diffusion coefficients are selected: $D = 2 \times 10^{-4}$ and $D = 10^{-3}$.

For the chosen values of the parameters the concentrations at the stationary state are equal to

$$V_s = 0.166\ 66, U_s = 4.710\ 35, E_s = 0.034\ 95,$$

$$X_s = 0.116\ 50$$

and the characteristic equation has two negative and two complex eigenvalues equal to

$$\lambda_1 = 1.963\ 16, \lambda_2 = -0.753\ 50, \lambda_3 = -0.005\ 73 +$$

$$0.006\ 44i, \lambda_4 = -0.005\ 73 - 0.006\ 44i$$

The homogeneous system exhibits excitability¹¹ for the above values of the rate constants and concentrations of S , R , and E_0 . We have verified by numerical calculations for finite in space systems with zero-flux boundary conditions that eqs 11–14 have solutions of a type of running impulse for properly chosen initial conditions.

To our best knowledge there are no theorems that allow for direct predictions of existence of asymptotic solutions of a set of reaction–diffusion equations in the form of the running impulses. Usually this form of asymptotic solutions is assumed in advance and next is verified in numerical calculations. Excitability itself is not sufficient to get the running impulse. Even if a system is locally excited, the pulse of excitation can decay because a back of it can move faster than its front. In order to shed light on the problem one can use arguments based on the Kanel theorem,^{19,20} which determines the existence of the running front solutions for one-variable reaction–diffusion equation for an infinite system. We will shortly explain below how this theorem can be used to argue that the running impulse type solutions can be expected for a set of coupled equations consisting of two reaction–diffusion equations (say, for variables α and β). Our approach is based on the assumption that α is a fast variable as compared with β . The similar assumption was used previously in construction of models for stationary periodical structures,²¹ trains of impulses,^{22,23} and standing waves²⁴ in chemical systems. Let us assume that for homogeneous conditions the equation for α has a N-shaped nullcline on the phase plane $\alpha \times \beta$. Assume next that a nullcline for β intersects the N-shaped nullcline at a left attracting branch, in such way that the system is excitable (see Figure 1). For sufficiently large initial local excitation of α one can argue that in fast time scale the variable β remains equal to its initial stationary value and a front of α will be formed and next spread with constant velocity according to the Kanel theorem. In the region left behind by the traveling front of α the distribution of β changes in slow time scale, and there the distribution of α as the fast variable is determined by the right attracting branch of the N-shaped nullcline. In this way a plateau of the distribution of α is formed because the front of α spreads over the slow time scale. At some instance, in the region of initial excitation the variable β reaches a minimal value allowed on the right attracting branch of the N-shaped nullcline, and at this moment one must return to the fast time scale in which the distribution of α joining right and left attracting branches of the N-shaped nullcline is formed. In this way a “back” of the impulse begin to form. Then β increases a little and eventually reaches a value at which a velocity of just formed “back” of the impulse becomes equal to the velocity of the running front formed previously. The impulse of α formed in the above way runs away from the region of the initial excitation, and if the velocities of the front and the back remain equal to each other then the running impulse spreads with constant velocity. In this case asymptotic solutions of the initial value problem for α and β have the form $\alpha(t, x) = \alpha(\xi)$ and $\beta(t, x) = \beta(\xi)$, where $\xi = x \pm ct$ and c denotes the velocity of the running impulse.

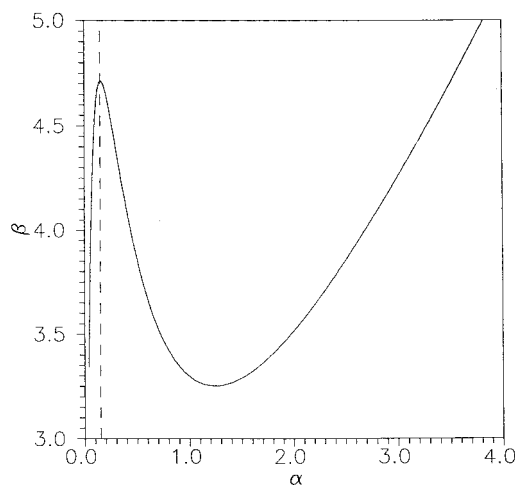


Figure 1. Schematic picture for the N-shaped nullcline for α and the nullcline for β (the dashed line).

For our model it is easy to check that if one assumes that the total concentration of catalyst (or the enzyme) E_0 is much smaller than the concentrations of V and U , then one can eliminate the variables E and X using the Tikhonov theorem,²⁵ and in this way one obtains the two-variable system with the N-shaped nullcline for V on the $V \times U$ plane. The nullcline for U intersects the N-shape nullcline in a point at which the system is excitable, and one obtains the model discussed above. Therefore, one can hope that for proper values of the parameters the solutions of our model will have the properties discussed above, namely, that the asymptotic solution of the corresponding initial value problem will have the form of running impulse for all four variables. These considerations have been verified by numerical calculations in which the initial value problem was replaced by the initial-boundary value problem with zero-flux boundary conditions. Solutions to this last problem are very good approximations of the initial value problem provided that the formed impulse is far from the boundaries of the system.

III. Master Equation

The mesoscopic treatment of a spatially extended (in one dimension) chemical system is an extension of this approach applied to the corresponding uniform system.¹¹ The system is divided into (let's say) M cells along the spatial coordinate; the volume Ω and the length Δl of each cell are identical. The state of our system is described by the probability distribution $P(\{N_{V,i}, N_{U,i}, N_{E,i}, N_{X,i}, N_{Y,i}\}, t)$ of finding a set of populations $N_{Q,i}$ of species $Q = V, U, E, X, Y$ in a cell $i = 1, \dots, M$. (A number of molecules R and S in each cell is assumed constant, equal to $N_R = R \cdot \Omega$ and $N_S = S \cdot \Omega$.) A number of molecules $N_{V,i}, N_{U,i}, N_{E,i}, N_{X,i}, N_{Y,i}$ in i th cell can be changed either by a chemical reaction between molecules within a cell or by a transfer of a molecule to or from adjacent cells. Both these processes independently contribute to the time evolution of the distribution function in the spatially extended system, and the master equation (ME) for P can be schematically written in the form

$$\frac{\partial P}{\partial t}(\{N_{V,i}, N_{U,i}, N_{E,i}, N_{X,i}, N_{Y,i}\}, t) = \frac{\partial P}{\partial t} \Big|_{\text{chem}} + \frac{\partial P}{\partial t} \Big|_{\text{diff}} \quad (19)$$

The contribution due to the chemical processes describes reactions that can involve only molecules in a single cell, provided that populations in other cells remain unchanged. It is a straightforward extension of the corresponding term in the

master equation for the uniform system¹¹

$$\begin{aligned} \frac{\partial P}{\partial t} \Big|_{\text{chem}} = & \sum_{j=1}^M (\kappa_1 N_R N_S P(\dots, N_{V_j} - 1, \dots, t) + \\ & \kappa_{-1} (N_{V_j} + 1) N_S P(\dots, N_{V_j} + 1, \dots, t) + \\ & \kappa_2 (N_{V_j} + 1) (N_{E_j} + 1) P(\dots, N_{V_j} + 1, \dots, N_{E_j} + 1, \dots, \\ & N_{X_j} - 1, \dots, t) + \kappa_{-2} (N_{X_j} + 1) N_S P(\dots, N_{V_j} - 1, \dots, \\ & N_{E_j} - 1, \dots, N_{X_j} + 1, \dots, t) + \\ & \kappa_3 (N_{X_j} + 1) N_S P(\dots, N_{U_j} - 1, \dots, N_{E_j} - 1, \dots, N_{X_j} + \\ & 1, \dots, t) + \kappa_4 (N_{V_j} + 1) (N_{X_j} + 1) P(\dots, N_{V_j} + \\ & 1, \dots, N_{X_j} + 1, \dots, N_{Y_j} - 1, \dots, t) + \\ & \kappa_{-4} (N_{Y_j} + 1) N_S P(\dots, N_{Y_j} + 1, \dots, N_{V_j} - 1, \dots, N_{X_j} - \\ & 1, \dots, t) + \kappa_5 (N_{V_j} + 1) N_S P(\dots, N_{V_j} + 1, \dots, N_{U_j} - 1, \dots, t) + \\ & \kappa_{-5} (N_{U_j} + 1) N_S P(\dots, N_{V_j} - 1, \dots, N_{U_j} + 1, \dots, t) - \\ & \nu_{\text{chem}} P(\{N_{V,i}, N_{U,i}, N_{E,i}, N_{X,i}, N_{Y,i}\}, t) \end{aligned} \quad (20)$$

The notation (\dots, N_{Q_j}, \dots) means that except N_{Q_j} all populations in the distribution function P remain unchanged. The positive components of the right-hand side of eq 20 describe creation of a given state, resulting from transitions from other states. The coefficient ν_{chem} provides the rate of escape from the configuration $\{N_{V,i}, N_{U,i}, N_{E,i}, N_{X,i}, N_{Y,i}\}$ as a result of any of chemical processes 1–5. Thus, it is given by the sum of the rates of all these chemical reactions:

$$\begin{aligned} \nu_{\text{chem}}(\{N_{V,i}, N_{U,i}, N_{E,i}, N_{X,i}, N_{Y,i}\}) = \\ \sum_{j=1}^M (\kappa_1 N_R N_S + \kappa_{-1} N_{V_j} N_S + \kappa_2 N_{V_j} N_{E_j} + (\kappa_{-2} + \kappa_3) N_{X_j} N_S + \\ \kappa_4 N_{X_j} N_{V_j} + \kappa_{-4} N_{Y_j} N_S + \kappa_5 N_{V_j} N_S + \kappa_{-5} N_{U_j} N_S) \end{aligned} \quad (21)$$

The coefficients κ_i are related to the rate constants k_i of reactions 1–5 by $\kappa_i = k_i/\Omega$. This relation ensures that the kinetic terms in eqs 6–10 can be recovered from eq 20 in the limit $\Omega \rightarrow \infty$, as the relations for the average concentrations $\langle N_{Q_j}/\Omega \rangle$.

It is assumed that every particle can jump with certain probability to a neighbor cell. These hoping rates are related to the diffusion coefficients and in general can be different for each species. The term of eq 19 describing diffusion has then the following form:

$$\begin{aligned} \frac{\partial P}{\partial t} \Big|_{\text{diff}} = \\ \sum_{j=1}^M (d_V (N_{V_{j-1}} + 1) P(\dots, N_{V_{j-1}} + 1, \dots, N_{V_j} - 1, \dots, t) + \\ d_V (N_{V_{j+1}} + 1) P(\dots, N_{V_j} - 1, \dots, N_{V_{j+1}} + 1, \dots, t) + \\ d_U (N_{U_{j-1}} + 1) P(\dots, N_{U_{j-1}} + 1, \dots, N_{U_j} - 1, \dots, t) + \\ d_U (N_{U_{j+1}} + 1) P(\dots, N_{U_j} - 1, \dots, N_{U_{j+1}} + 1, \dots, t) + \\ d_E (N_{E_{j-1}} + 1) P(\dots, N_{E_{j-1}} + 1, \dots, N_{E_j} - 1, \dots, t) + \\ d_E (N_{E_{j+1}} + 1) P(\dots, N_{E_j} - 1, \dots, N_{E_{j+1}} + 1, \dots, t) + \\ d_X (N_{X_{j-1}} + 1) P(\dots, N_{X_{j-1}} + 1, \dots, N_{X_j} - 1, \dots, t) + \\ d_X (N_{X_{j+1}} + 1) P(\dots, N_{X_j} - 1, \dots, N_{X_{j+1}} + 1, \dots, t) + \\ d_Y (N_{Y_{j-1}} + 1) P(\dots, N_{Y_{j-1}} + 1, \dots, N_{Y_j} - 1, \dots, t) + \\ d_Y (N_{Y_{j+1}} + 1) P(\dots, N_{Y_{j+1}} + 1, \dots, N_{Y_j} - 1, \dots, t) - \\ \nu_{\text{diff}} P(\{N_{V,i}, N_{U,i}, N_{E,i}, N_{X,i}, N_{Y,i}\}, t) \end{aligned} \quad (22)$$

In this equation, the terms for boundary cells, $j = 1$ and M , are

determined by boundary conditions. For impermeable walls, what is the case considered here, transitions of molecules outside the system are forbidden. The coefficient ν_{diff} , describing the total rate of diffusive jumps for all cells, can be written as:

$$\begin{aligned} \nu_{\text{diff}}(\{N_{V,i}, N_{U,i}, N_{E,i}, N_{X,i}, N_{Y,i}\}) = \\ d_V N_{V,1} + d_U N_{U,1} + d_E N_{E,1} + d_X N_{X,1} + d_Y N_{Y,1} + \\ 2 \sum_{j=2}^{M-1} (d_V N_{V_j} + d_U N_{U_j} + d_E N_{E_j} + d_X N_{X_j} + d_Y N_{Y_j}) + \\ d_V N_{V,M} + d_U N_{U,M} + d_E N_{E,M} + d_X N_{X,M} + d_Y N_{Y,M} \end{aligned} \quad (23)$$

The relation between the transition rates d_Q and the diffusion coefficients D_Q follows from the condition that the diffusion flux of the component Q , $-A \cdot D_Q \Delta n_Q / \Delta l$ (where A is a surface of a cross section of a cell), is obtained from the average value of the net transition rate of Q between adjacent cells. This yields the relation $d_Q = D_Q / (\Delta l)^2$, which shows that for a given value of the macroscopic diffusion coefficient the hoping rates d_Q increase for finer divisions.

The master equation gives the description of the stochastic system in terms of the probability distribution function. From equivalent point of view, the stochastic dynamics can be considered as a random walk of an individual system. In the case of our system, it is the random motion in a discrete space, where coordinates of each point correspond to a specific configuration of populations $\{N_{Q,i}\}$ in cells. We have performed simulations of this (continuous time) random walk applying the method of Gillespie²⁶ to generate a stochastic trajectory. Let us assume that the system at an instant t is in a state which is given by the point $\{N_{V_j}, N_{U_j}, N_{E_j}, N_{X_j}, N_{Y_j}\}$. The total rate of escape of the system from this point due to any reaction or diffusion process is equal to $\nu = \nu_{\text{chem}} + \nu_{\text{diff}}$. According to this, in the first step of the algorithm, a waiting time τ for the transition is sampled from the exponential distribution with the mean ν^{-1} . The next step consists of choosing a particular reaction or diffusion process, which causes a transfer of the system to another point. The probability $p(\alpha)$ of selection of process α (reaction or diffusion in a j th cell) is proportional to its contribution to the total rate of escape ν . For chemical reaction ρ in a cell j , that means

$$p_{\text{chem}}(\rho, j) = \nu^{-1} \kappa_\rho N_{1\rho,j} N_{2\rho,j} \quad (24)$$

where $N_{1\rho,j}$, $N_{2\rho,j}$ denote populations of molecules of two species involved in the bimolecular reaction ρ . Similarly, for the probability of a diffusive jump (to the left or right) of a molecule Q in a cell j one obtains

$$p_{\text{diff}}(Q, j) = \nu^{-1} d_Q N_{Q,j} \quad (25)$$

Next, the populations $\{N_{V_j}, N_{U_j}, N_{E_j}, N_{X_j}, N_{Y_j}\}$ are updated as they result from the chosen process α ; in terms of the random walk the system moves to the new point. Given this new state, generation of dynamics proceeds beginning from the first step, and so on.

IV. Results and Discussion

Our main interest is in comparison between the deterministic behavior given by the solutions of the reaction–diffusion equations and the stochastic description obtained from the simulations of the master equation. However, we were able to perform efficient simulations of the master equation for systems with total number of particles of the order of 10^6 . Concentra-

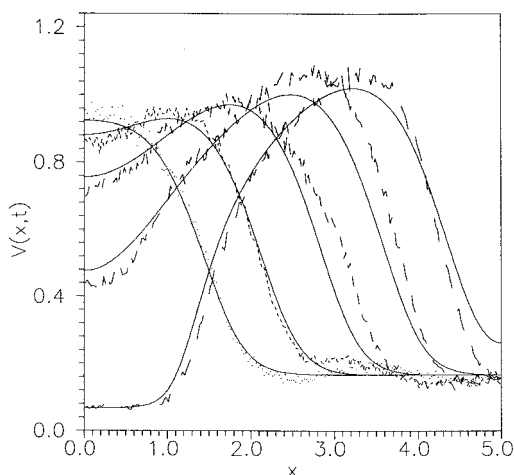


Figure 2. Snapshots of the distributions of V in the system divided into $M = 200$ cells of the volume $\Omega = 5 \times 10^{-6}$ (in μm^3) with $D = 10^{-3}$ (in $\mu\text{m}^2/\mu\text{s}$) at times (in μs): $t = 200$ (the points), 400 (the very short dashed line), 600 (the short dashed line), 800 (the dashed line), and 1000 (the long dashed line). The corresponding numerical solutions of the reaction–diffusion equations (eqs 11–14) are shown as solid lines.

tions of reagents in real chemical mixtures are of the order of $1\text{ mol}/\text{dm}^3$, and thus a simulated system with such numbers of particles cannot have a macroscopic size. Therefore, the unit of length we use throughout the paper is $1\text{ }\mu\text{m}$. We study the finite system of length $l = 5\text{ }\mu\text{m}$. The length of a cell is uniquely determined by a number of cells used in division of a system of given length. Also the time scale in simulations cannot have usual units (order of seconds). The unit of time we use in this paper is $1\text{ }\mu\text{s}$. The concentrations are expressed in usual units of mol/dm^3 .

The master equation approach can be expected to be valid if the results of simulations using different system divisions are consistent, which means they are independent of value of M chosen for a given length of the system. We have verified in the previous paper¹⁴ on the trigger wave propagation in the system of the same length, that the divisions into $M = 200$ and 400 cells give correct results of simulations. It is not necessary to apply finer divisions, for which the computing time required for simulations increases, owing to higher rate of diffusive jumps between thinner cells. Therefore, in simulations performed here we use the above two values of M for divisions of the system.

Two values of the diffusion coefficient equal to 2×10^{-4} and 10^{-3} (in $\mu\text{m}^2/\mu\text{s}$) are used. In usual units of cm^2/s these coefficients are equal to 2×10^{-6} and 10^{-5} , respectively. These values of D are of the same order as in real fluids.

In order to simulate a formation of the running impulse, we excite initially the system in the interval $[0,1]$ (in μm) assuming $V = 1.0$ and $U = 3.5$, whereas the other concentrations are the same as in the stationary state. In the remaining part of the system all concentrations have the stationary values V_s , U_s , E_s , X_s , and Y_s . In ME simulations the corresponding populations of molecules in each cell are determined from the condition that N_α/Ω are equal to the above deterministic concentrations.

In Figure 2 we compare the distributions of V in the system with faster diffusion, $D = 10^{-3}$, obtained for times $t = 200, 400, \dots, 1000$ (in μs) from the numerical solutions of the deterministic reaction–diffusion equations (eqs 11–14) and from the ME simulations. The system is divided into $M = 200$ cells of the volume $\Omega = 5 \times 10^{-6}$ (in μm^3). For this value of D the running impulse, when it is developed, is so wide that it almost does not have enough room in the system of the

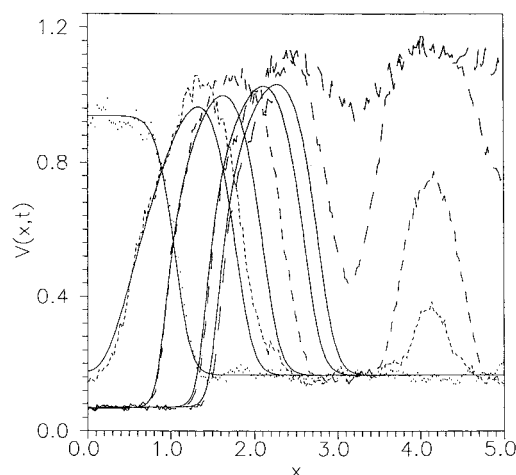


Figure 3. Snapshots of the distributions of V in the system divided into $M = 200$ cells of the volume $\Omega = 5 \times 10^{-6}$ (in μm^3) with $D = 2 \times 10^{-4}$ (in $\mu\text{m}^2/\mu\text{s}$) at times (in μs): $t = 100$ (the points), 600 (the very short dashed line), 800 (the short dashed line), 1100 (the dashed line), and 1200 (the long dashed line). The corresponding numerical solutions of the reaction–diffusion equations (eqs 11–14) are shown as solid lines.

assumed length l . Quite good agreement is seen between the deterministic evolution and the stochastic simulations for shorter times, when the front of the impulse is developed and V at the left boundary is falling down. The difference between the results of the two approaches becomes larger for longer times. It is due to excitations close to the front of the impulse, which affect its propagation by changing its instantaneous velocity. In Figure 2 such fluctuation at the leading edge of the front is seen for $t = 400$, and one can notice that it subsequently induces a large shift of the front position for $t = 600$. This influence resembles effects observed in simulations of one-variable models of chemical fronts^{16,17} for which it is even possible to determine the diffusive spread of the front around its average (deterministic) position.¹⁶ We have observed the similar effect in the propagation of the trigger wave¹⁴ described by the reduced version of the scheme in eqs 1–5. Fluctuations are much less significant at the back of the impulse, where the strong deterministic dynamics prevails. Indeed, one can see in Figure 2 that the agreement between the stochastic and deterministic description for long times is better for the back of the impulse than for its front. The concentrations of all reagents in the uniform region seen behind the running impulse are not equal to the stationary values. As follows from the results for the homogeneous system,¹¹ the time needed to return after excitation to the stationary state is above 3000, which is much longer than we can reach in ME simulations in this paper.

Figures 3–5 show the snapshots of distributions of V obtained by numerical solutions of eqs 11–14 and by the ME simulations with the diffusion coefficient $D = 2 \times 10^{-4}$. In Figures 3 and 4 the ME simulations are performed for the same $\Omega = 5 \times 10^{-6}$ (in μm^3) but for $M = 200$ and $M = 400$, respectively, whereas Figure 5 shows results for $\Omega = 8.33 \times 10^{-6}$ and $M = 400$. According to the deterministic predictions, the impulse moves slower and becomes sharper when the diffusion coefficient is smaller. This effect can be observed by comparing Figures 3 and 2, which depict results for the same system but with different diffusion coefficients $D = 2 \times 10^{-4}$ and 10^{-3} , respectively. This relation is also confirmed in stochastic simulations. As in the previous case, agreement between the deterministic evolution and the ME simulations is relatively good during the initial period, for which fluctuations affect only

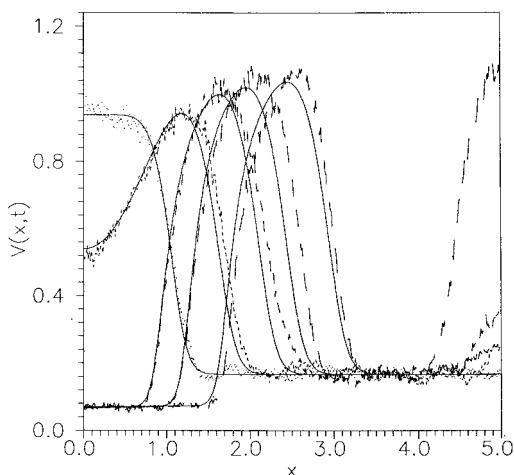


Figure 4. Snapshots of the distributions of V in the system divided into $M=400$ cells of the volume $\Omega = 5 \times 10^{-6}$ (in μm^3) with $D = 2 \times 10^{-4}$ (in $\mu\text{m}^2/\mu\text{s}$) at times (in μs): $t = 100$ (the points), 500 (the very short dashed line), 800 (the short dashed line), 1000 (the dashed line), and 1300 (the long dashed line). The corresponding numerical solutions of the reaction–diffusion equations eqs 11–14 are shown as solid lines.

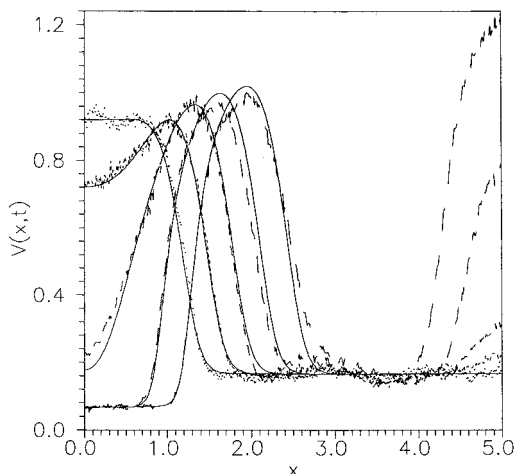


Figure 5. Snapshots of the distributions of V in the system divided into $M = 400$ cells of the volume $\Omega = 8.33 \times 10^{-6}$ (in μm^3) with $D = 2 \times 10^{-4}$ (in $\mu\text{m}^2/\mu\text{s}$) at times (in μs): $t = 200$ (the points), 400 (the very short dashed line), 600 (the short dashed line), 800 (the dashed line), and 1000 (the long dashed line). The corresponding numerical solutions of the reaction–diffusion equations (eqs 11–14) are shown as solid lines.

front propagation velocity. This is the effect similar to that seen in Figure 2. Additional, qualitatively different effects of fluctuations can be seen in the system with slower diffusion. Diffusion introduces coupling between adjacent cells, and therefore, fluctuations in individual cells are not independent. The slower is diffusion, the coupling extends over smaller distance, and domains of excitations can easier grow to macroscopic size. In this way fluctuations generate spontaneous impulses of excitation in the region ahead of the initial impulse. After such impulse is created, it expands according to the wave mechanism and can collapse with the original front. This is an essential difference in comparison with the system with the higher diffusion coefficient. Spontaneous creation of such impulses is a purely stochastic effect, which is excluded in the phenomenological description. Such effects are seen at a later period of the stochastic evolution. Local excitations are more probable close to the right boundary (see Figures 4 and 5), because the smoothing effect of diffusion is weaker at an

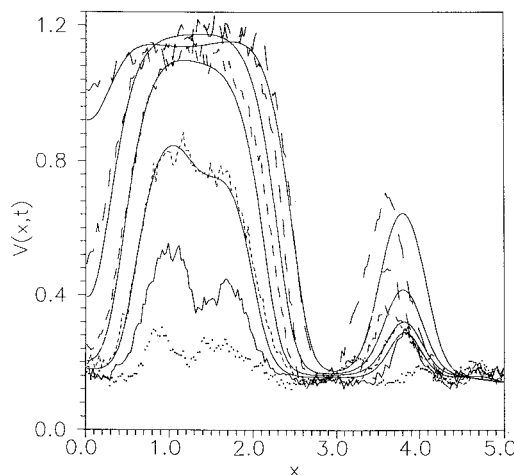


Figure 6. Snapshots of the distributions of V in the initially homogeneous system with the same parameters as in Figure 3 at times (in μs): $t = 400$ (the points), 600 (the solid line), 700 (the very short dashed line), 800 (the short dashed line), 900 (the dashed line), and 1000 (the long dashed line). The distribution at $t = 600$ was used as the initial condition in numerical solutions of the reaction–diffusion equations (eqs 11–14), which are shown as solid lines at the corresponding times.

impermeable wall (fluctuation are there spread only in one direction). However, they are not excluded also at some distance from the boundary (see Figure 3). The simulations of the homogeneous excitable system¹¹ have shown that fluctuations grow more easily in a system with smaller volume. This effect is also seen in Figure 3 and 4, which present the results obtained for the systems in which only volumes of cells are different. Most of the system with a smaller cell is excited at time $t = 1200$ (see Figure 3), whereas a much smaller region became excited at $t = 1300$ in Figure 4 for larger cells.

Fluctuations are able to excite locally the system that at initial time has uniform distributions of all reagents. Development of such local excitations needs longer time intervals than those used in simulations of the running impulse discussed above. We could not reach these times in ME simulations for higher diffusion coefficient with our computer facilities. Evolution of local excitations in the system characterized by $D = 2 \times 10^{-4}$, $M = 200$, and $\Omega = 5 \times 10^{-6}$ is depicted in Figures 6 and 7. Until $t = 400$, fluctuations were not able to induce local excitations that could survive. The snapshot for $t = 400$ shows the initial stage of formation of the excitations, which have just passed the “critical value”. The right excitation is smaller, less developed than the left one. In order to compare the further stochastic evolution with the deterministic behavior we assumed the distributions of all reagents at $t = 400$ as the initial conditions for the reaction–diffusion equations, (eqs 11–14). The results of numerical solutions were in quite good agreement in the left part of the system, but the excitation at $x = 4$ did not survive. These solutions are not shown in Figure 6. The deterministic prediction is incorrect in this case because in a range of concentrations close to the stationary state the deterministic dynamics is weak, and therefore fluctuations are relatively more important. We have obtained much better agreement between the stochastic evolution and numerical solutions of eqs 11–14 if the distributions of all reagents at $t = 600$ are chosen as the initial condition. These results are shown in Figure 6. The agreement in the left part of the system is very good, but the most right excited domain obtained in ME simulations is slightly shifted to the left with respect to the deterministic profile. The later period of the stochastic evolution up to decaying of

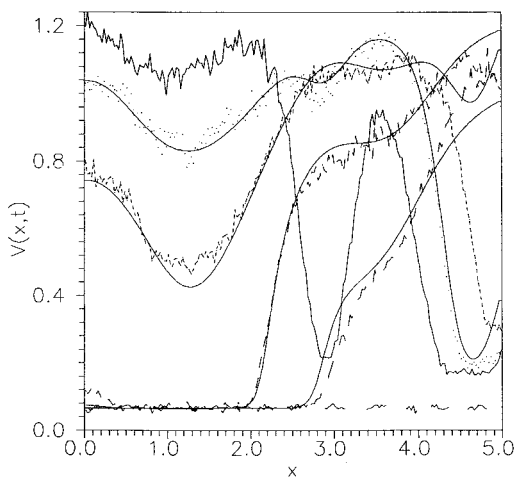


Figure 7. Continuation of the results presented in Figure 6. Snapshots of the distributions of V are shown at times (in μs): $t = 1100$ (the solid line), 1300 (the points), 1500 (the very short dashed line), 1700 (the short dashed line), 1900 (the dashed line), and 2400 (the long dashed line). The distribution at $t = 1100$ was used as the initial condition in numerical solutions of the reaction–diffusion equations (eqs 11–14), which are shown as solid lines.

excitation is shown in Figure 7. The very good agreement between the results of ME simulations and deterministic evolution is obtained if the distributions of all reagents for $t = 1100$ are taken as initial conditions for eqs 11–14. For sufficiently long time, $t = 2400$, the whole system becomes uniform, which is consistent with the deterministic result. If the distributions of concentrations are sufficiently far from their stationary values, then they are in strong vector direction field determined by the phenomenological equations and small fluctuations do not influence significantly the dynamics of the system. This is the reason why the deterministic description gives satisfactory approximation to the ME simulations in such cases. The situation is completely different if the concentrations distributions are close to the stationary state where the vector direction field is weak. In this case fluctuations become the dominant factor that governs the dynamics of the system, and the deterministic description fails.

There is no direct relation between our model and realistic mechanisms of the B–Z reaction and other excitable systems. Nevertheless, the results of our ME simulations can be helpful in explanation of the old but still not completely solved problem of a character of sources of target patterns observed in the B–Z system.²⁷ Two different concepts have been taken into account in phenomenological description of these patterns. Heterogeneous sources (pacemakers) are small regions with parameters different from those in the bulk.^{1,28–31} Such heterogeneities can increase frequency of oscillations (in oscillatory regime) or they can induce localized Hopf bifurcation from excitable to oscillatory regime in excitable system. Homogeneous sources (leading centers) describe the same effects, but only local perturbations of reagents concentrations are allowed and the target patterns appear owing to intrinsic chemical dynamics.^{32–38} The ME approach allows a stochastic description of the target patterns that appear in excitable systems. In order to simulate the target patterns, the size of the system must be much larger than that considered here because it has to allow for generation of the tail of the impulse where the next spontaneous excitation is possible. This condition means also much longer time of simulations. Let us assume now that at some instant a first excitation is generated in some place and the next two running impulses spread from it. Other excitations can also appear later

on in a region that is not reached by the first impulse. The place of the first excitation returns to a neighborhood of the stationary state earlier than regions that became excited later, and therefore, it has a good chance to be excited again before other places. In this way the next pair of running impulses could be generated there, and this place becomes the leading center. The same scenario occurs in the regions that were excited later. All places in which excitations were generated appear to be in an apparently oscillatory regime with a “period” of oscillations of order of the “return time”, and all of them become sources of impulses. Since the return time has some distribution, one can expect that subsequent running impulses generated by each source will not be equidistant, but this effect can be really small if the distribution is sharp.

V. Conclusions

Our results of ME simulations show that internal fluctuations can induce local excitations that strongly disturb the behavior predicted by phenomenological dynamics for spatially extended excitable systems. Fluctuations not only affect the velocity and shape of the running impulses but they can also generate new spontaneous excitations that interact with the earlier developed impulse. In this way larger regions of the system become excited than predicted by solutions of the corresponding reaction–diffusion equations.

The comparison of the results of ME simulations performed for homogeneous (ideally stirred) excitable systems, in which only global fluctuation are possible,¹¹ with the results presented in this paper shows that local fluctuations have much stronger influence on the behavior of the spatially extended systems. The spatially extended system is excited more easily than the well-stirred system with a similar number of molecules. The reason for this is that in the extended system excitations can occupy initially only a small part of the system. Such localized fluctuations are much more easily created than perturbation of the system as a whole, and they can survive if diffusion is sufficiently slow. Therefore, the phenomenological description that does not include fluctuations seems to be much more satisfactory for the well-stirred systems than for the spatially extended ones. On the other hand, if concentration distributions are locally sufficiently far from stationary values, then the phenomenological description based on reaction–diffusion equations is in reasonable agreement with the stochastic dynamics.

As one can expect, an enlargement of the diffusion coefficient increases the velocity and the width of the running impulse. These properties have been observed in numerical solutions of the phenomenological equations as well as in our ME simulations. Moreover, the higher diffusion coefficient makes the appearance of excitations more difficult.

It is noteworthy that our chemical model is simple and realistic, and therefore, it indicates that it should be possible to find simple real systems, in which the influence of fluctuations can be tested experimentally. The crucial steps correspond directly to the Langmuir–Hinshelwood (or the Michaelis–Menten) kinetics to which an inhibition by excess of the reactant is added. Such schemes have been used to describe kinetics of many enzymatic reactions.

Acknowledgment. This work was supported by the Grant KBN 3T09A 120 08 provided by the Polish State Committee for Scientific Research.

References and Notes

- (1) See, for example: Zhabotinsky, A. M. *Concentrations Autooscillations*; Nauka: Moscow, 1974 (in Russian). Field, R.J.; Burger, M.

Oscillations and Travelling Waves in Chemical Systems; Wiley: New York, 1985. Murray, D. J. *Mathematical Biology*; Springer Verlag: Berlin, 1989. Gray, P.; Nicolis, G.; Baras, F. *Spatial Inhomogeneities and Transient Behaviour in Chemical Kinetics*; Manchester University Press: Manchester, 1990. Kawczyński, A. L. *Chemical Reactions from Equilibrium through Dissipative Structures to Chaos*; WN-T: Warsaw, 1990 (in Polish).

- (2) Field, R.J.; Noyes, R.M. *J. Am. Chem. Soc.* **1974**, *96*, 2001.
- (3) Ortoleva, P.; Schmidt, S. In *Oscillations and Traveling Waves in Chemical Systems*; Field, R. J., Burger, M., Eds.; Wiley: New York, 1985; p 333.
- (4) Kuhnert, L.; Krug, H. *J. Chem. Phys.* **1987**, *91*, 730.
- (5) Ševčíkova, H.; Marek, M. *Phys. D* **1983**, *9*, 140.
- (6) Wood, P. M.; Ross, J. *J. Chem. Phys.* **1985**, *82*, 1924.
- (7) Nagy-Ungvarai, Z.; Tyson, J. J.; Hess, B. *J. Phys. Chem.* **1989**, *93*, 707.
- (8) Nicolis, G.; Prigogine, I. *Self-Organization in Non-equilibrium Systems*; Wiley: New York, 1977.
- (9) van Kampen, N. G. *Stochastic Processes in Physics and Chemistry*; North-Holland: Amsterdam, 1983.
- (10) Gardiner, C. W. *Handbook of Stochastic Methods*; Springer-Verlag: Berlin, 1985.
- (11) Nowakowski, B.; Gorecki, J.; Kawczyński, A. L. Submitted to *J. Phys. Chem.*
- (12) Kawczyński, A. L.; Gorecki, J.; Nowakowski, B. Submitted to *J. Phys. Chem.*
- (13) Gorecki J.; Gryko J. *Comput. Phys. Commun.* **1989**, *54*, 245.
- (14) Nowakowski, B.; Kawczyński, A. L. *Acta Phys. Pol. B* **1997**, *28*, 2057.
- (15) Baras F.; Malek Mansour M. *Adv. Chem. Phys.* **1997**, *100*, 393.
- (16) Breuer, H.-P.; Huber, W.; Petruccione, F. *Europhys. Lett.* **1995**, *30*, 69. Breuer, H.-P.; Huber, W.; Petruccione, F. *Physica D* **1994**, *73*, 259.
- (17) Karzazi, M. A.; Lemarchand, A.; Mareschal, M. *Phys. Rev. E* **1996**, *54*, 4888.

(18) Zel'dovich, Ya. B.; Mikhailov, A. S. *Fiz. Nauk* **1987**, *153*, 469 (in Russian) and references therein.

- (19) Kanel, Ya. I. *Mat. Sb.* **1962**, *59*, 243 (in Russian).
- (20) Fife, P. C. *Mathematical Aspects of Reacting and Diffusing Systems*; Springer: Berlin, 1979.
- (21) Górski, J.; Kawczyński, A. L. *Pol. J. Chem.* **1985**, *59*, 61.
- (22) Górski, J.; Kawczyński, A. L. *Pol. J. Chem.* **1983**, *57*, 187.
- (23) Kawczyński, A. L. *Pol. J. Chem.* **1986**, *60*, 223.
- (24) Kawczyński, A. L. *Pol. J. Chem.* **1989**, *63*, 611.
- (25) Tikhonov, A. N. *Mat. Sb.* **1952**, *31*, 574 (in Russian).
- (26) Gillespie, D. T. *J. Phys. Chem.* **1977**, *81*, 2340.
- (27) Zhabotinsky, A. M.; Zaikin, A. N. *J. Theor. Biol.* **1973**, *40*, 45.
- (28) Ortoleva, P.; Ross, J. *J. Chem. Phys.* **1974**, *60*, 5090.
- (29) Tyson, J. J.; Fife, P. C. *J. Chem. Phys.* **1980**, *73*, 2224.
- (30) Kopell, N. *Adv. Appl. Math.* **1981**, *2*, 389. Kopell, N.; Howard, L. *Adv. Appl. Math.* **1981**, *2*, 417.
- (31) Bugrim, A. E.; Dolnik, M.; Zhabotinsky, A. M.; Epstein, I. R. *J. Phys. Chem.* **1996**, *100*, 19017.
- (32) Vasilyev, V. A.; Zaikin, A. N. *Kinet. Catal.* **1976**, *17*, 903 (in Russian).
- (33) Zaikin, A. N.; Kawczyński, A. L. *J. Non-equilib. Thermodyn.* **1977**, *2*, 39.
- (34) Kobayashi, R.; Ohta, T.; Hayase, Y. *Phys. Rev. E* **1994**, *50*, R3291.
- (35) Zhabotinsky, A. M.; Dolnik, M.; Epstein, I. R. *J. Chem. Phys.* **1995**, *103*, 10306.
- (36) Sakaguchi, H. *Prog. Theor. Phys.* **1992**, *87*, 241.
- (37) Mikhailov, A.S. *Physica D* **1992**, *55*, 99.
- (38) Borckmans, P.; Dewel, G.; De Wit, A.; Walgraef, D. In *Chemical Waves and Patterns*; Kapral, R., Showalter, K., Eds.; Kluwer: Dordrecht, 1995; p 323.